

THE HILBERT-HUANG SPECTRAL ANALYSIS METHOD APPLIED TO VIV

Celso P. Pesce¹
(ceppesce@usp.br)

André L.C. Fuarra²
(afuarra@usp.br)

Leonardo K. Kubota²
(leonardo.kubota@poli.usp.br)

LIFE&MO - Fluid-Structure Interaction and Offshore Mechanics Laboratory

¹Department of Mechanical Engineering

²Department of Ocean Engineering

Escola Politécnica
University of São Paulo
São Paulo, SP, Brazil

ABSTRACT

Vortex-Induced Vibration (VIV) is a highly nonlinear dynamic phenomenon. Usual spectral analysis methods rely on the hypotheses of linear and stationary dynamics. A new method envisaged to treat nonlinear and non-stationary signals was presented by Huang et al. [1] : *The empirical mode decomposition and the Hilbert spectrum for nonlinear and non-stationary time series analysis*. This technique, called thereafter the Hilbert-Huang transform (or spectral analysis) method, is here applied to VIV phenomena, aiming at disclosing some hidden dynamic characteristics, such as the time-modulation and jumps of multi-branched response frequencies and their related energy spectra.

Keywords: VIV, analysis techniques, Hilbert transform, Empirical Mode Decomposition.

NOMENCLATURE

D	Cylinder diameter
L	Cylinder length
$m^* = 4m / \rho\pi D^2 L$	Mass ratio
m	Structural mass
m_A	Added mass

$C_A = 4m_A / \rho\pi D^2 L$	Added mass coefficient
ζ or $\zeta^S = c / c_{cr}$	Structural damping coefficient
U	Flow velocity
Re	Reynolds number
$V_r = U / f_y D$	Reduced velocity
f_y or f_{ny}	Natural frequency in transverse direction in still water
A_y	VIV transverse amplitude response
x_1 and y_1	Stream and cross-wise directions of vibration for the upstream cylinder
x_2 and y_2	Stream and cross-wise directions of vibration for the downstream cylinder

INTRODUCTION

Vortex-Induced Vibration (VIV) is a highly nonlinear dynamic phenomenon and a very important topic that has been addressed by many investigators, under numerical, empirical and phenomenological models. As VIV is still an open subject in fluid-structure interactions, it certainly reserves much more discussion in the riser dynamics scenario; see, e.g., Pesce and Martins [2] .

Experimental or numerical time-histories that emerge from VIV investigation are bound to be, in essence, nonlinear and non-stationary. In the marine riser scenario, in stratified currents at very low values of mass ratio and damping coefficients, a rich dynamic behavior appears, where many branches of amplitude and frequency responses, multi-modal excitation, jumps, sub-harmonic resonance, mode switching and bifurcations of vortex shedding patterns may exist, making the analysis extremely difficult. On the other hand, usual spectral analysis methods rely on the hypotheses of linear and stationary dynamics.

A new method envisaged to treat nonlinear and non-stationary signals was presented by Huang et al. [1] : *The empirical mode decomposition and the Hilbert spectrum for nonlinear and non-stationary time series analysis*. This technique, called thereafter the Hilbert-Huang transform method (H-H), is here applied to VIV phenomena, aiming at disclosing some hidden dynamic characteristics, such as the time-modulation and jumps of multi-branched response frequencies and their related energy spectra. Examples of some time-series analysis are shown, emphasizing jumps, responses in increasing (decreasing) velocity regimes and dynamic responses related to wake interferences of a tandem arrangement.

It should be mentioned that the Hilbert transform has already been applied in the VIV context to study the intermittent switching vibration that may occur between the lower and upper branches responses; Govardhan and Williamson [3] . In that case, however, the Hilbert transform is applied directly to the signals, without decomposing it into mode functions. In the H-H technique, the signal is first decomposed into Intrinsic Mode Functions (IMF) and each of them is then treated through the Hilbert transform. This will be addressed in more details.

SOME NON-STATIONARY VIV PROBLEMS IN WATER

Vortex-induced Vibration (VIV) is a key matter in the design of marine structures, particularly in the fatigue life evaluation of catenary risers.

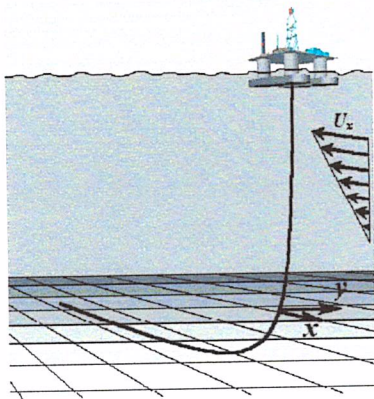


Figure 1 A typical steel catenary riser.

Many very complex issues, as modal competition (and modulation due to cyclic tension) in stratified and multi-

directional current profiles, challenge researchers and engineers. Nevertheless, VIV remains an open research subject, where fundamental matters are still under strong investigation; see, e.g., Williamson and Govardhan [4] .

Among those, one of the most significant topics, relevant to the riser scenario, is the two degrees-of-freedom (in- and out-of-plane) dynamics at low values of mass and damping ratios that characterizes this kind of marine structure. Jauvtis and Williamson [5] , in their comprehensive experimental study with a pendulum-like, rigid cylinder apparatus, have definitely shown the large effect that the stream-wise oscillations may cause in the transverse vibration. This happens at mass ratios m^* less than 6. Usually, marine risers present m^* of order 2.0 to 3.0.

In their work, Jauvtis and Williamson studied what they called 'the super-upper branch' of VIV response, relating it to their striking finding: a new vortex-shedding mode, the 2T mode, where a triplet of vortices is shed each half-cycle. The transverse amplitude response at the 'super-upper' branch is by far larger (circa 50%) than the typical maximum value attained in x-restrained experiments. Nevertheless, despite some other efforts in close related areas suggesting the importance of two degrees-of-freedom effects, most design practices and codes applied in offshore engineering rely on direct extrapolations of results of studies with just one degree-of-freedom that usually give amplitudes of circa one diameter.

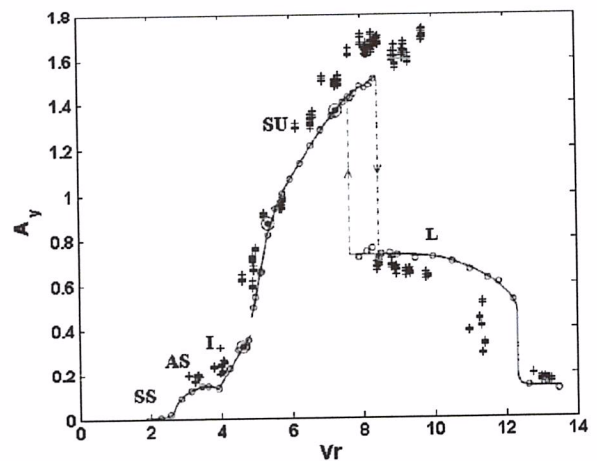


Figure 2 VIV transverse amplitude response of a flexible cantilevered cylinder, acquired at the tip (+), more details in Pesce and Fujarra [7] [8] , $m^* = 2.4$; $(m^* + C_A)\zeta = 0.016$, compared with the rigid cylinder apparatus results (o), $m^* = 2.6$; $(m^* + C_A)\zeta = 0.013$, Jauvtis and Williamson [5] .

As can be noticed from Figure 2, the importance of Jauvtis and Williamson findings, for the rigid cylinder, should be emphasized in the flexible cylinder scenario. This figure, by Fujarra and Pesce [7] , simply compares some of the key results obtained with the rigid cylinder apparatus, with another and previous one, Pesce and Fujarra [8] , obtained with a flexible

and long cantilevered cylinder in water. In this latter experiment a large aspect ratio flexible cylinder was towed in a 280 m long, 6.0 m wide and 4.5 m deep, towing tank facility, at $Re \approx 6,000 - 40,000$, fully exciting the first flexural vibration mode. It is more than remarkable the neat similarity existent between both experimental results, despite the distinct setups and instrumentation techniques used. Apart some small differences, at the response peak and at the end of the lower branch, all points characterizing the initial (I) and the ‘super-upper’ (SU) branches match extremely well.

Besides an unusual large transverse amplitude response peak, the flexible cantilevered cylinder exhibited jumps, at $U_r \approx 8.3^1$, from the ‘lower branch’ to what we may recognize as a ‘super-upper branch’. This particular phenomenon will be analyzed and discussed through the application H-H technique.

In the riser scenario, the possible existence of high modal amplitude responses of order of 1.5 to 2 diameters, related to the bifurcation of the vortex-shedding pattern from the classical 2P to the new 2T mode, could then be inferred. This certainly would have an impact on fatigue life evaluation, particularly in the touchdown area (TDA); see Pesce et al. [9].

Sub-harmonic resonance driven by this coupling between stream and cross-wise oscillations is another phenomenon that should be further investigated. It should be pointed out that, for catenary-risers, the eigenfrequencies corresponding to in-plane and out-of-plane modes always appear interlaced one after the other. Therefore, for a given reduced velocity range, the occurrence of rational ratios between stream and crosswise frequencies, leading to the appearance of complex multi-branched amplitude responses, would always be possible. According to Sarpkaya [10], page 61, ratios other than 2 lead to “considerably more complex” responses. Figure 3 gives an example of a sub-harmonic resonance for a very flexible cantilevered cylinder, taken from Fuarra et al. [11].

The secondary branch in the transversal response that appears at high-reduced velocity is caused by a sub-harmonic resonance driven by the stream-wise oscillation and may be triggered by structural impact or upstream wake disturbance. The first triggering mechanism might be caused by risers clashing; the second one, by a simple wake interference of an upstream riser. Both phenomena are very likely to occur in full-scale. Should such secondary branches be excited, fatigue life evaluation would be highly impacted. The sub-harmonic resonance phenomenon, shown in Figure 3, will be also analyzed through the H-H spectral analysis technique.

Other complex transient dynamics in VIV, of substantial importance for riser dynamics, may be cited, such as those related to wake interference between cylinders.

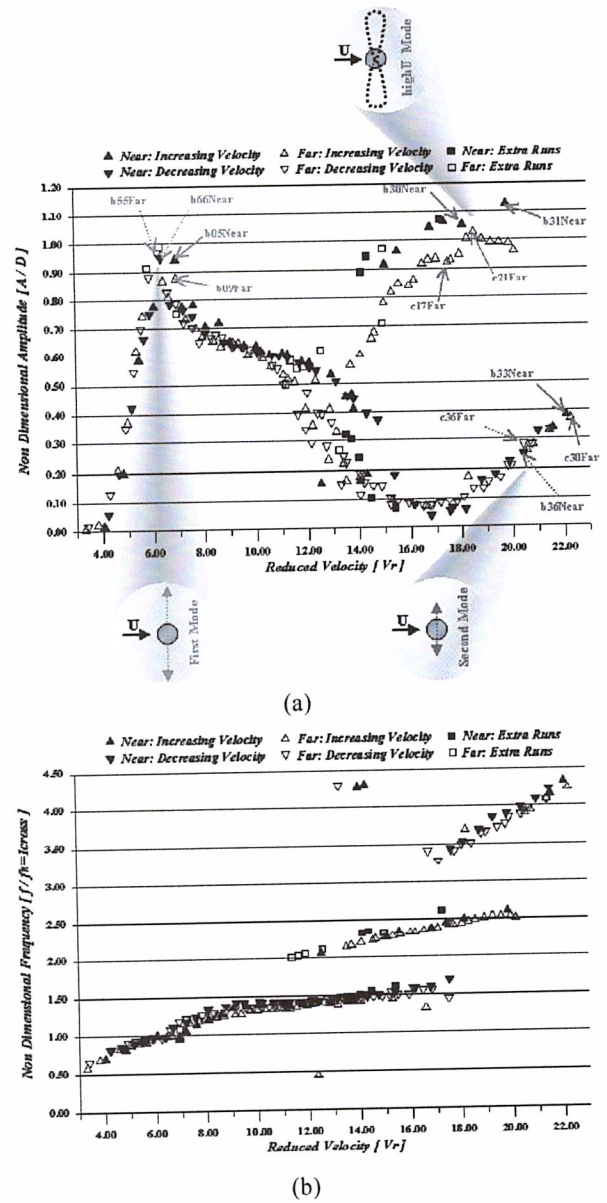


Figure 3 VIV transversal amplitude (a) and frequency (b) of a flexible cylinder. Sub-harmonic resonance and frequencies driven by stream wise oscillation; $m^*=1.36$; $(m^* + C_a)(\zeta_{1y}^S)_{water} = 0.034438$. The “near” and “far” conditions are related to the distance between the tip and the bottom of the water channel. The first and second mode motions are in the cross-flow direction and the third (high-U mode) is a coupling between stream and cross-wise response.

¹ Reduced velocity is calculated as $U_r = U/f_y D$, where f_y is the natural frequency in transverse direction in still water.

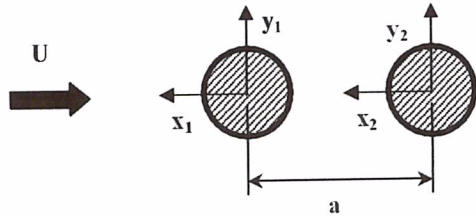


Figure 4 Two equal cylinders in tandem arrangement.

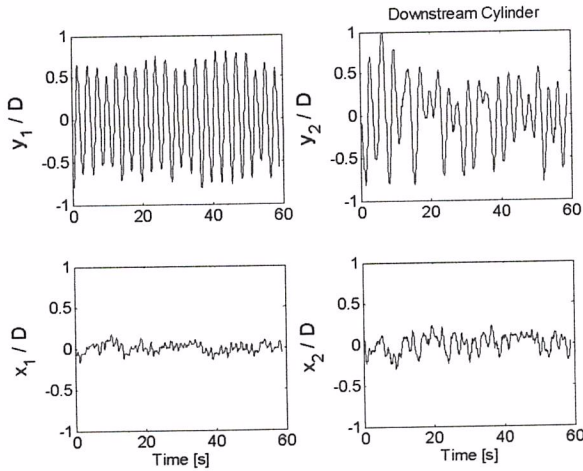


Figure 5 Stream (x) and crosswise (y) vibrations of two cylinders in tandem arrangement. $I_r^* = U/f_y D = 12$; $D = 75\text{mm}$; $a = 2.5D$.

This phenomenon is an example of a typical situation for which the usual spectral analysis may be questionable. In fact, depending on the clearance between cylinders in a tandem arrangement, the downstream cylinder (and even both cylinders) may experience strongly non-stationary oscillations.

A particular sample of results is shown in Figure 5, for a typical tandem arrangement, shown in Figure 4. The H-H technique will be also applied for this particular example.

The revealed dynamic behavior scenario is indeed quite reach, where different types of dynamic bifurcations may be present, possibly leading to chaotic vibration and to clashing. This is due to inherent wake instabilities caused by fluid-structure interactions; see, e.g., Herfjord and Bryndum [12], Sagatun et al. [13], Wu et al. [14], Huang and Wu [15].

Another interesting possible application of the H-H technique is on the data obtained in a set of experiments with a vertical tensioned flexible pipe in stratified current, reported by Chaplin et al. [16]. Those experiments revealed many interesting non-stationary dynamic behaviors, including “significant contributions from several modes, all at the same frequency” and mode switching. As a matter of fact, as reported by those authors: “...the riser’s response was found to be quite sensitive to disturbances in the ambient conditions; a mechanical shock or the presence of an old wake in the

incident flow were sometimes enough to promote a sudden switching of modes”.

THE HILBERT- HUANG SPECTRUM TECHNIQUE

The Hilbert-Huang spectrum analysis was envisaged and developed by Huang et al. [1] as an alternative and powerful technique to deal with non-stationary signals that emerge from non-linear systems. This method applies the usual Hilbert transform to a finite set of ‘Intrinsic Mode Functions’² (IMFs), obtained from the original signal through an ‘Empirical Mode Decomposition’ (EMD). According to those authors: “the name ‘intrinsic mode function’ is adopted because it represents the oscillation mode imbedded in the data”.

Let $X_j(t)$ be a specific IMF and $Z_j(t)$ an analytic function defined as

$$Z_j(t) = X_j(t) + iY_j(t) = a_j(t) \exp[i\theta_j(t)] \quad (1)$$

where

$$Y_j(t) = \frac{1}{\pi} P \int_{-\infty}^{\infty} \frac{X_j(\tau)}{t - \tau} d\tau \quad (2)$$

is the Hilbert Transform of $X_j(t)$; P stands for principal value.

The original signal is then decomposed into the IMF set, as in a ‘generalized Fourier series’,

$$X(t) = \text{Re} \sum_{j=1}^n a_j(t) \exp\left(i \int \omega_j(t) dt\right), \quad (3)$$

in the sense that not only the amplitude $a_j(t)$ but also the local phase $\theta_j(t)$, and so the local (or instantaneous) frequency,

$$\omega_j(t) = \frac{d}{dt}(\theta_j(t)), \quad (4)$$

of each IMF, is time dependent. The concept of local frequency can be formalized through the stationary phase method, as pointed out in [1].

The EMD method, conceived to obtain the set of IMFs, is based on a recursive subtraction of successively calculated mean between the two time-envelope of extrema (maxima and minima) that are contained in the signal. The envelopes are splines fitting of the maxima (and minima). Details can be found in [1], where this method is referred to as a ‘sifting’ process. Such a recursive procedure is carried out for each IMF limited by a standard deviation stopping criterion that is applied at each step. Each calculated IMF has, itself, symmetrical (maxima and minima) envelopes. The IMF set is complete, by construction. The orthogonality property was shown numerically in [1]. The residual function coming out from this procedure is not an IMF; it is the (long-term) trend of the signal. The method precludes zero or mean references and is applicable to general transient signals.

² In the H-H technique, the intrinsic “mode” is a temporal one, not the structural “mode” (vibration eigenmode).

THE H-H TECHNIQUE APPLIED TO VIV: SOME EXAMPLES

Three examples will be shown: (a) a typical jumping signal; (b) a decreasing velocity experiment along a sub-harmonic resonance branch (and an increasing-decreasing velocity run along a usual lower-branch); (c) wake interference VIV experiment of two cylinders in tandem.

The jumping phenomenon

We apply the H-H technique to the typical jumping signal shown in Figure 6, obtained for a long flexible cylinder at a reduced velocity $U_r \approx 8.3$, from the 'lower to the super-upper branch'; see Figure 2.

Figure 7 shows the original signal together with six IMFs and the residual (trend) function. Note that, in this case, the first IMF almost recovers the whole information of the original signal. The fact that the original signal envelope is almost symmetrical around a zero mean could explain this. The first IMF, of large energy, carries the most important features. The higher the IMF the lower is the typical range of oscillation frequency. The lower frequencies are intrinsic in the amplitude modulation. In this case, the higher the IMF, the lower is also the energy. Figure 8 presents the H-H spectrum for the first three (most energetic) IMFs. The upper plot presents the reduced velocity time-history together with the time-traces corresponding to each IMF. The lower plot shows the corresponding amplitude envelopes. We can observe the frequency jump of the first IMF, at $t \approx 15$ s, corresponding to the branch jump. The frequency is higher (~ 2.5 Hz) in the lower amplitude branch and lower (~ 2 Hz) in the upper one, as should be expected, from common physical arguments.

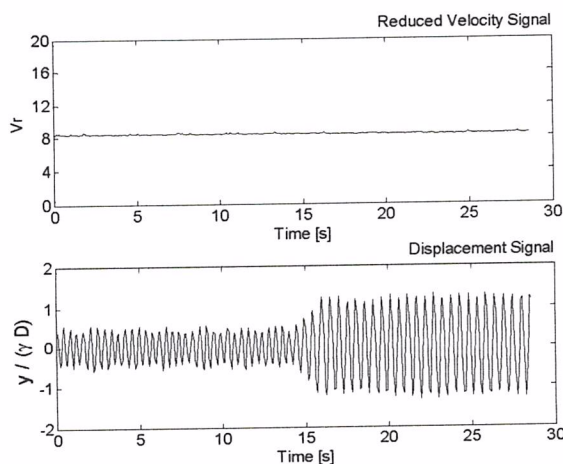


Figure 6 Jump of transversal VIV of a long flexible cantilevered cylinder, adapted from Pesce and Fujarra [7] ; (a) reduced velocity; (b) transverse amplitude response. The amplitude jumps at $U_r \approx 8.3$ (see Figure 3).

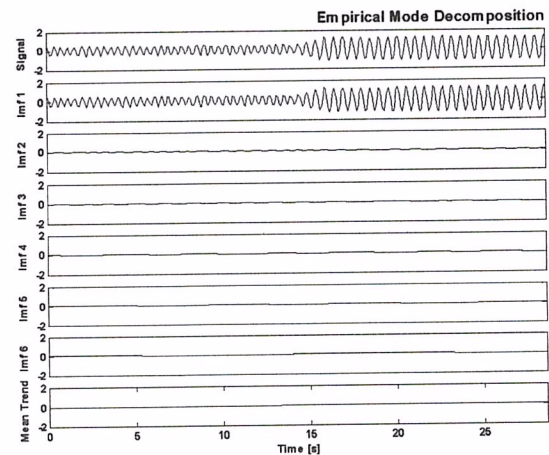


Figure 7 Original signal and six Intrinsic Mode Functions (IMF) for the signal shown in Figure 6. Note that the lower plot is the trend, not an IMF.

The fluctuation of both, the amplitude and the frequency time-traces, is smaller for the upper amplitude branch, an evidence of a better synchronization. Spikes of frequency for the third IMF, around $t \sim 25$ s, could be attributed to rapid variations of IMF 3, a low energy mode. The physical interpretation of this event is not clear, though.

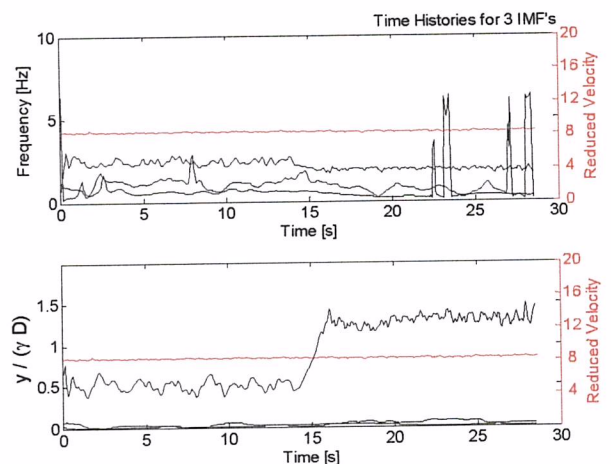


Figure 8 Frequency and amplitude H-H spectrum corresponding to three IMFs shown in Figure 7.

Figure 9 shows the same information in a single colored map. Traces corresponding to the IMFs other than the first are almost indistinguishable, as they are much less energetic. The H-H spectrum clearly depicts two distinct regimes with a certain degree of stationarity. In this particular example, the transient part of the signal is confined between 15-16 s, a very narrow window of time. It seems reasonable to isolate the distinct regimes and to apply linear spectral analysis, as shown in Figure 10. The fundamental frequencies are, respectively, 2.5 and 1.9 Hz, recovering the time-averaged frequencies that may be obtained from Figure 9.

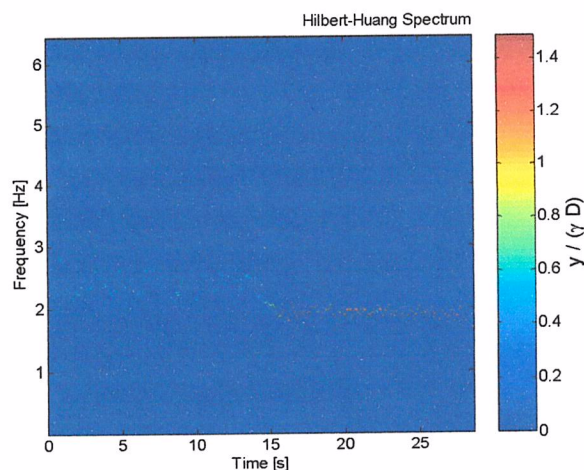


Figure 9 Colored Hilbert-Huang Spectrum corresponding to IMFs shown in Figure 7. Only the spectrum of IMF #1 is distinguishable. The other two are of very low amplitude.

Therefore, this particular case does not fully demand the H-H technique. Apart from the jump time-window, conventional analysis may be applied. Nevertheless, the clear information on frequency and amplitude modulations, obtained from the H-H technique, would be lost.

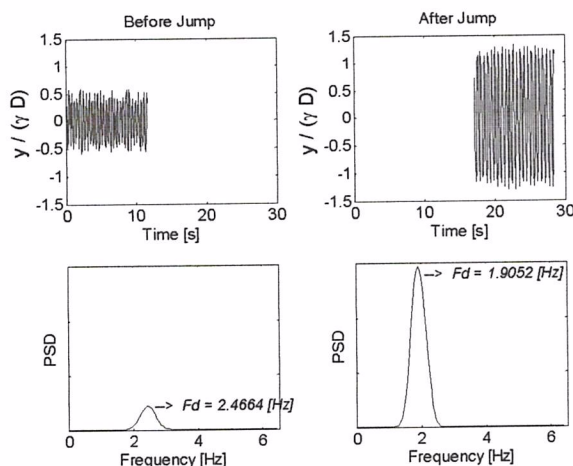


Figure 10 Usual Power Spectrum Density analysis taking two pieces of the whole signal as stationary excerpts, before and after the jumping.

Sub-harmonic resonance and mode switching in increasing and decreasing velocities

We now exemplify the application of the H-H technique to the VIV of a very flexible cylinder with two quite distinct flexural rigidities in the stream and crosswise planes. The cantilever comprises a leaf spring encased within a rubber flexible cylinder, restricting the vibrations of the body in a water channel flow to principally transverse motion; see details

in Fajarra et al.[11]. The two distinct rigidities enable a sub-harmonic resonance to be triggered by structural or upstream wake disturbances, as shown in Figure 3. This vibration mode is due to a strongly coupled stream and crosswise motion, where the stream wise amplitude becomes non-negligible. Such a sub-harmonic resonance mode presents large transverse amplitudes and follows a branch that merges with the usual lower branch response, at its end, at a reduced velocity $I_r^* \approx 12$. The high, stable and auto-sustained resonance branch ceases at $I_r^* \approx 20$, after the second transverse flexural mode of vibration is fully excited, destroying the wake synchronism that couples the stream-wise vibration.

Figure 11 shows a typical decreasing transverse amplitude signal along the sub-harmonic branch, starting at $I_r^* \approx 16$ and ending at $I_r^* \approx 10$; see Figure 3, for reference. Some important aspects should be emphasized. The first one is the clear change in resonance behavior at $t \sim 100$ s when $I_r^* \approx 12$. As may be seen from Figure 3, $I_r^* \approx 12$ corresponds to the point where the sub-harmonic resonance branch merges the plateau of the usual lower-branch, and is dominated by it, which is induced by the well-known 2P vortex-shedding wake pattern.

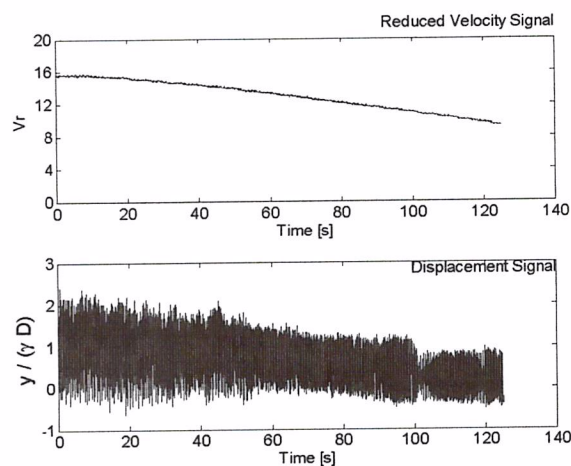


Figure 11 Transverse oscillation of a very flexible cylinder along a sub-harmonic resonance branch, entering the lower branch in decreasing velocity.

The second point deserving a special comment is the average drifting of the signal, obtained from strain-gages measurements. Note that the presented signal is the originally one and has non-zero mean. The drift is caused by a non-symmetric (torsional-flexural) bending of the cantilevered cylinder, due to the mean drag, which is dependent on the velocity. These two points testify to a non-stationary signal³. Figure 12 shows the original signal and the corresponding set of eight IMFs. Figure 13 shows their colored H-H spectrum.

³ This kind of signal is very likely to occur in field experiments.

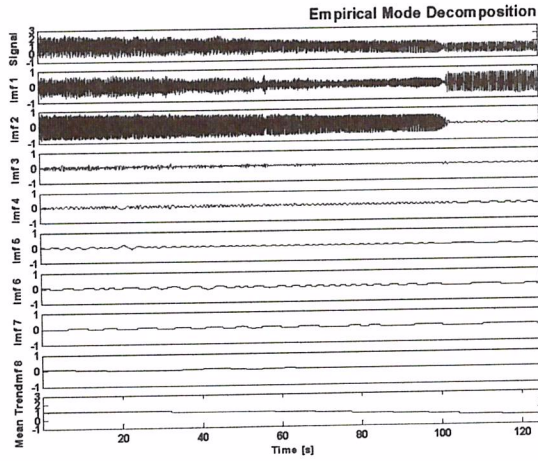


Figure 12 Original signal and eight Intrinsic Mode Functions (IMF) for the signal shown in Figure 11. Note that the lower plot is the trend (the average drift), not an IMF.

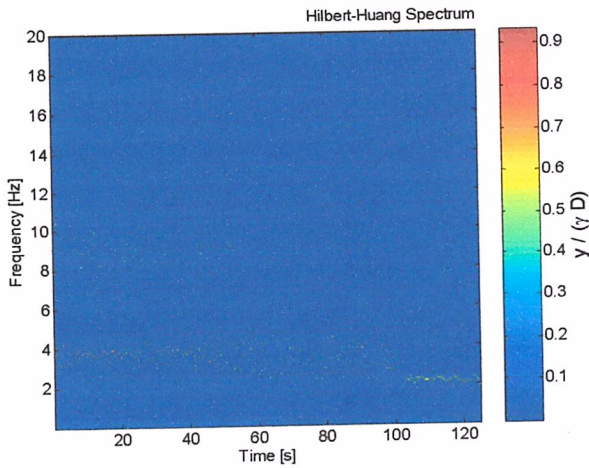


Figure 13 Colored Hilbert-Huang Spectrum corresponding to IMFs shown in Figure 12.

From $t \sim 0$ to $t \sim 100$ s, IMF 1 and 2 present the same level of amplitude. In other words, two distinct hydro-elastic oscillation modes co-exist, each of them represented in time by a distinct IMF. IMF1 corresponds to the fundamental oscillation frequency that lies in the range 3 - 4 Hz, and follows the lower frequency plot in Figure 3.

IMF 2 is clearly related to the sub-harmonic (x-y coupled) resonance branch, characterized by higher frequencies, of order 9 - 10 Hz, and follows the intermediate frequency plot in Figure 3. It is now even clearer the abrupt change of oscillatory behavior that occurs at $t \sim 100$ s. At this instant, when the sub-harmonic resonance branch merges to the lower branch, IMF 1 and 2 change abruptly as well as their corresponding frequency time-traces. In other words, the sub-harmonic resonance mode ceases, dominated by the usual lower branch mode that abruptly gains energy and continues to grow as the reduced velocity is decreased.

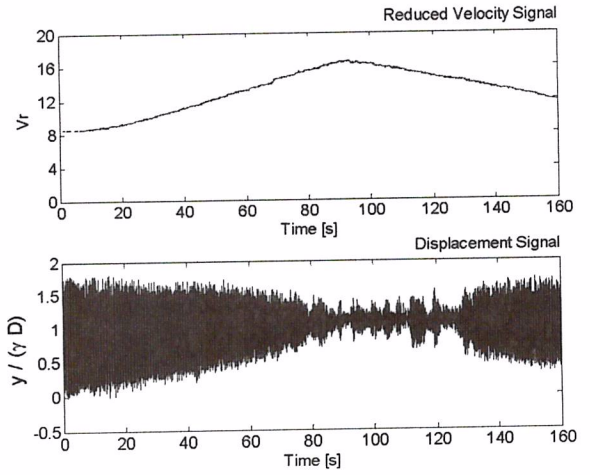


Figure 14 Transverse oscillation of a very flexible cylinder along the main (usual) dynamic response, during an increasing-decreasing velocity run.

Figure 14 shows an increasing-decreasing velocity run, starting at $V_r \approx 8$, going up to $V_r \approx 16$ and going down again to $V_r \approx 12$; see Figure 3. Similarly, to the signal presented in Figure 11, the mean is not zero, though the slow drift is less perceptible in this case. Figure 15 presents the original signal and the corresponding set of 8 IMFs, while Figure 16 shows their colored H-H spectra.

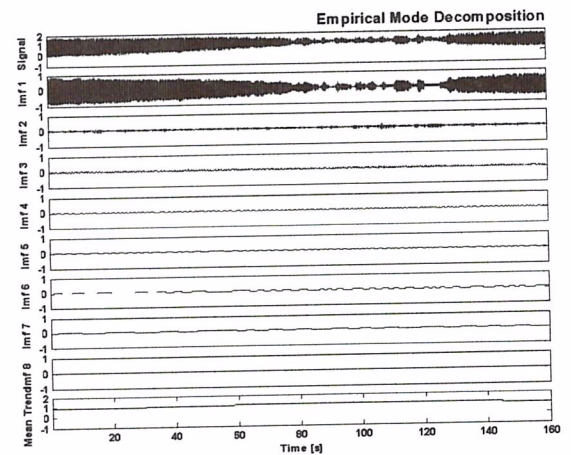


Figure 15 Original signal and eight Intrinsic Mode Functions (IMF) for the signal shown in Figure 14. Note that the lower plot is the trend (the mean and drift), not an IMF.

In this case the run followed the main (usual) amplitude response curve, from the beginning of the lower branch to the end of the lock-in of the first flexural mode. The sub-harmonic response branch was not triggered. IMF 1 is the most energetic and contains the relevant information. The frequency time-trace corresponding to IMF 1 corresponds to the lower frequency plot in Figure 3. The frequency increases as the reduced velocity increases (and the transverse amplitude decreases) -

and conversely, in the decreasing velocity regime. As expected, the oscillation frequency time-trace is more sparse (less defined) in the colored map when the transverse amplitude is lower, i.e., outside the lock-in range. This happens, in this run, in the time interval $80s \leq t \leq 130s$, corresponding to reduced velocities in the interval $14 \leq U_r \leq 16$ - and where the signal and the IMF 1 are much more intermittent.

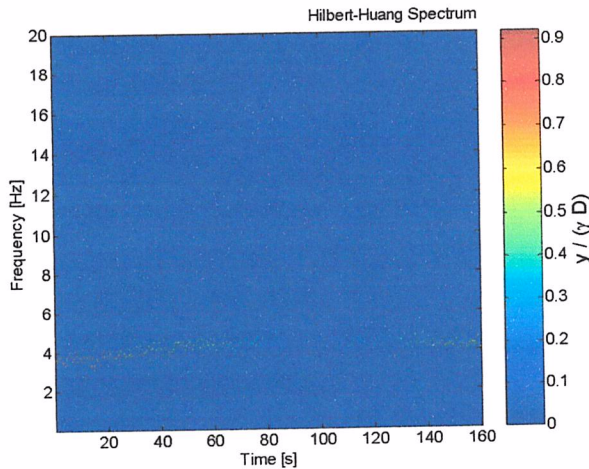


Figure 16 Colored Hilbert-Huang Spectrum corresponding to IMFs shown in Figure 15.

Note, once more, that all IMFs are constructed in such way as to have zero mean. Therefore, the corresponding amplitude information refers to the dynamics, only. A non zero-mean (either electrical or physical) is automatically separated as well as the drifting.

Two cylinders in tandem

We turn our attention to the samples exemplified in Figure 5, from an experimental run with two identical cylinders in tandem arrangement. The experiments were carried out at the same towing tank used for the first flexible cylinder experiment, for many clearance values.

The plots depicted in Figure 5 are typical samples, corresponding to a clearance $a = 2.5D$ under a towing carriage speed of 0.2 m/s ($U_r \approx 12$). The diameter of the cylinders is $D = 75\text{mm}$ and the natural frequencies *in still water*, for both, in stream and crosswise directions were measured as 0.33 and 0.23 Hz , respectively⁴. The total sample time is 60 s . The time series are relatively short due to the limitations imposed by the towing tank length.

As may be noticed from Figure 17-20, only the crosswise oscillation of the upstream cylinder may be seen as presenting a certain degree of stationarity, though with a clear modulation. The crosswise oscillation of the downstream cylinder is clearly non-stationary and larger than the first one. The stream-wise oscillations of both, the upper and the downstream cylinders, are strongly non-stationary, though relatively small, if

compared to the crosswise oscillations. The towing tank carriage velocity presented some fluctuation, possibly causing spurious vibration response.

It is clear, for the stream-wise oscillations, that the energy is much more equally distributed among the IMFs. Actually, IMFs 3-7 concentrate the important information. The corresponding frequency time-traces extend up to 1.6 Hz . Lower frequencies are related to the modulations in amplitude and phase and their time-traces present strong fluctuations.

By observing the crosswise oscillations, it is clear that the energy is, in this case, much more concentrated in few IMFs. Particularly, one IMF concentrates the relevant information in the upstream cylinder oscillations, practically recovering the original signal. Consequently, the corresponding frequency time-trace is very energetic but presents small fluctuations around 0.35 Hz . This is a measure of stationarity. The amplitude modulation is clear from the other frequency time-traces. On the other hand, the crosswise oscillation of the downstream cylinder is much more distributed among three distinct IMFs. This result is consistent with its highly non-stationary nature. The most energetic frequency time-trace fluctuates more than the corresponding one for the upstream cylinder. However, the modulating slow-frequencies, corresponding to the other two IMFs, fluctuate as much as those for the upstream cylinder do.

PERSPECTIVES AND CONCLUDING REMARKS

The present paper addressed the application of the Hilbert-Huang spectral analysis technique to some typical VIV problems where non-stationarity and non-linearity are quite evident. In such cases, the application of common linear spectral analysis techniques, which rely on strong hypotheses of stationarity and linearity, is strongly questionable. Other techniques suitable for non-stationary signals, like wavelet analysis, e.g., [17] [18], or complex demodulation, [19], are also based on linearity. Actually, wavelet analysis has been used as a reference method, by Huang et al. [1], to validate their technique. Nevertheless, wavelet results are usually 'blurred', if compared to those obtained through the H-H analysis. Moreover, the H-H method is able to treat non-zero mean signals with strong drifting, leaving to the empirical mode decomposition the proper treatment of this issue. In addition, as pointed out by Huang et al. [1], "the introduction of the Hilbert spectrum also provides a quantitative measure of the degree of stationarity".

In the present paper, we firstly applied the H-H technique to some interesting VIV phenomena. Single jumps and switching between distinct hydro-elastic vibration modes, coexistence of distinct vibration modes, as well as VIV affected by the wake interference between cylinders, were analyzed. Interesting dynamic features, referring to energy distribution, amplitude and frequency modulation were disclosed. We believe that, at the present stage, a deeper analysis of the intrinsic mode functions and their H-H spectra may help to construct a more complete physical interpretation of complex phenomena involved in VIV and VIM (vortex-induced motion).

⁴ Note the ratio, $0.33/0.23 \sim 3/2$.

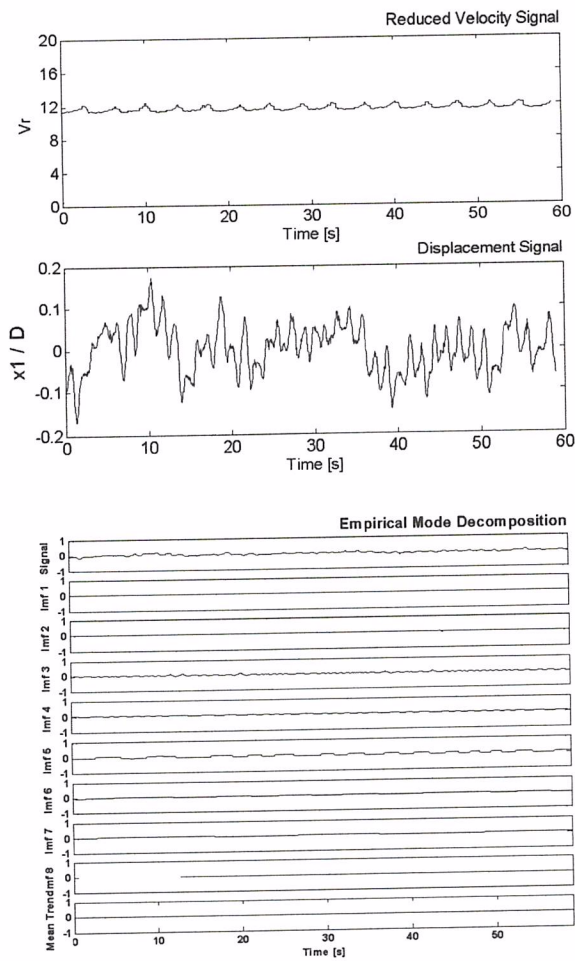


Figure 17 Stream wise oscillations of the upstream (x_1) cylinder, respective IMFs and H-H spectrum.

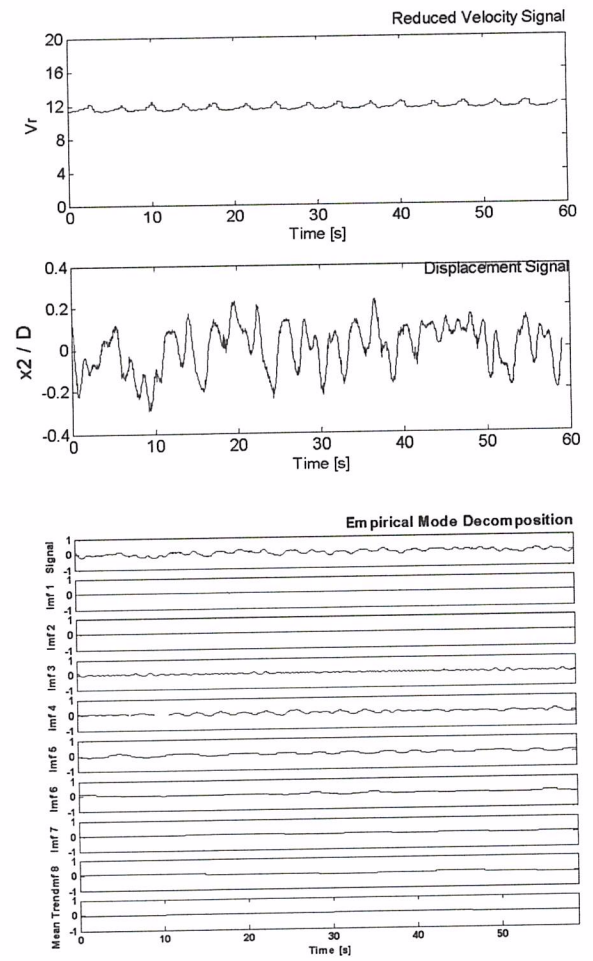
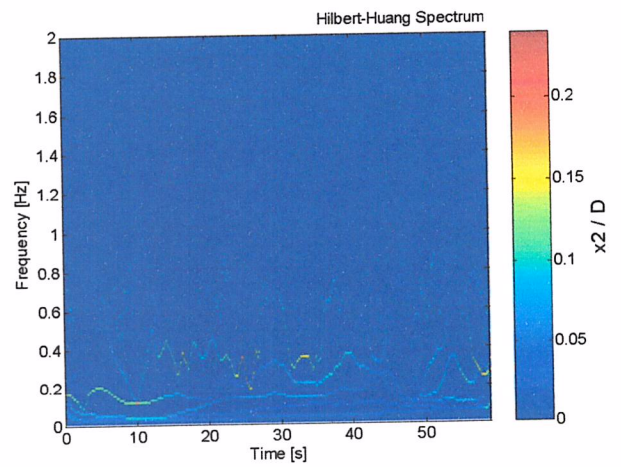
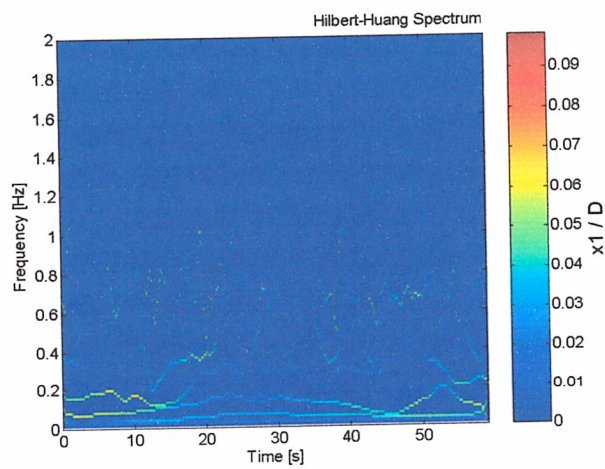


Figure 18 Stream wise oscillations of the downstream (x_2) cylinder, respective IMFs and H-H spectrum.



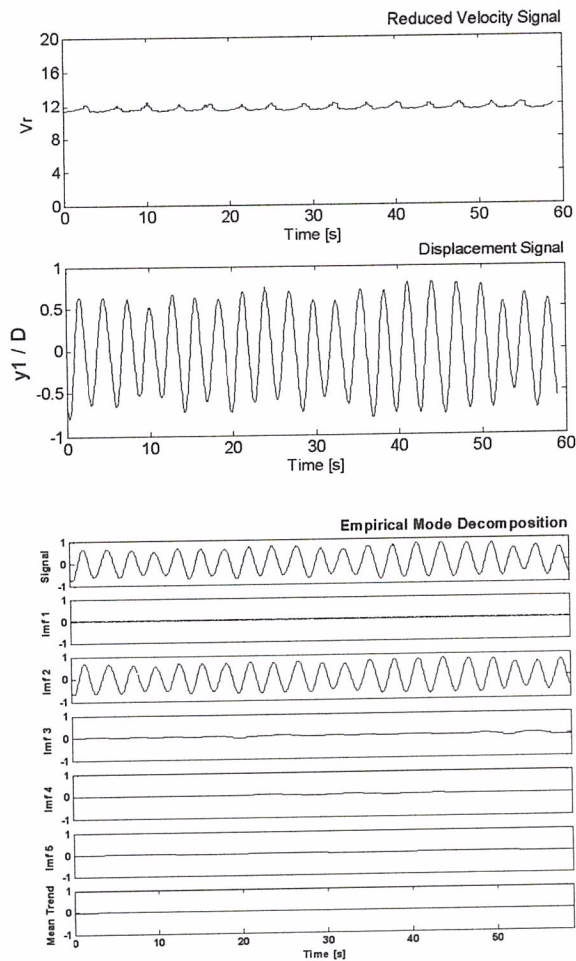


Figure 19 Crosswise oscillations of the upstream (y_1) cylinder, respective IMFs and H-H spectrum.

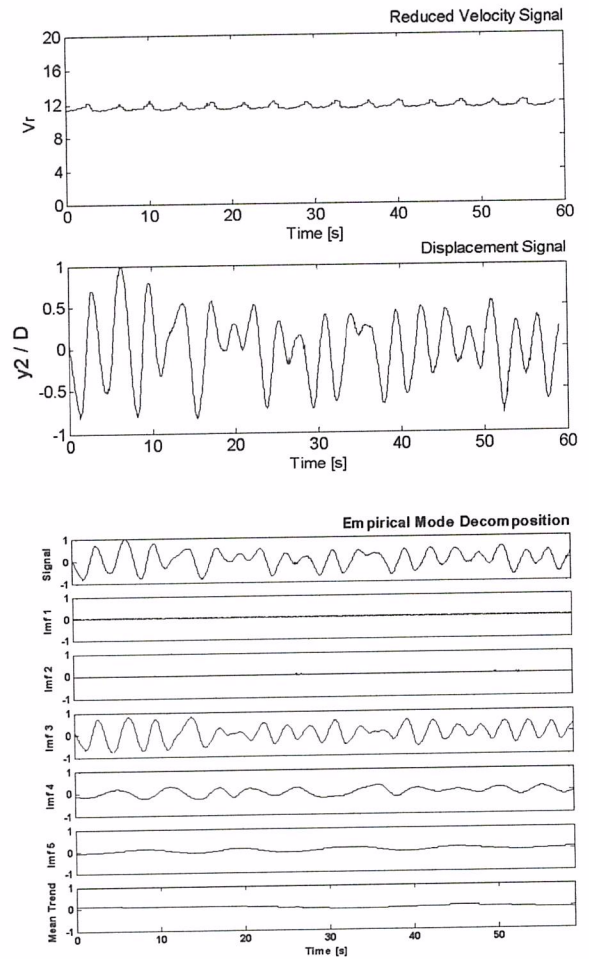


Figure 20 Crosswise oscillations of the downstream (y_2) cylinder, respective IMFs and H-H spectrum.

A further, deeper and more comprehensive investigation is certainly needed. Coupling of VIV with linear and non-linear dynamics in other time-scales is another source of potential transient phenomena that might be analyzed through the H-H technique. For example, tension oscillation in different time-scales, related to first and second-order wave-motions of the floating unit (FU), may trigger mode excitation and multi-mode switching of vibrating catenary risers. The H-H technique might then help the analysis of full-scale VIV measurements and monitoring, complementarily to usual methods of analysis.

ACKNOWLEDGMENTS

This work has been supported by ANP, the Brazilian Petroleum National Agency, Program PRH-19 and FAPESP, the State of São Paulo Research Agency, process 03/12330-3. Research grants from CNPq, National Research Council, process 302450/2002-5 and FINEP, process 2882/04, are also acknowledged. We thank PETROBRAS for the continuing support in riser dynamics and VIV research, particularly Dr. Ricardo Franciss.

REFERENCES

- [1] Huang, N.E. et al, 1998, "The Empirical Mode Decomposition and the Hilbert Spectrum for Non-linear and Non-stationary Time Series Analysis", *Proc. R. Soc. Lond. A*, **454**, pp. 903-995.
- [2] Pesce, C.P. and Martins, C.A., 2005, "Numerical Computation of Riser Dynamics", Chapter 7 in *Numerical Modeling in Fluid-Structure Interaction*, Ed. S. Chakrabarti, WIT Press, Southampton, UK, Chapter 7, pp. 253-309.
- [3] Govardhan, R. and Williamson, C.H.K., 2000, "Modes of Vortex Formation and Frequency Response of a Freely Vibrating Cylinder", *J of Fluid Mechanics*, **420**, pp. 85-130.
- [4] Williamson, C.H.K. and Govardhan, R., 2004, "Vortex-Induced Vibrations", *Annual Rev. Fluid Mech.*, **36**, pp. 313-455, 2004.
- [5] Jauvtis, N. and Williamson, C.H.K., 2004, "The Effect of Two Degrees of Freedom on Vortex-Induced Vibration at Low Mass and Damping", *J Fluid Mechanics*, Vol. 509, pp. 23-62.
- [6] Kim, W.J. and Perkins, N., 2002, "Two-dimensional Vortex-induced Vibration of Cable Suspensions", *J Fluids and Structures*, **16**, pp. 229-245, 2002.
- [7] Pesce, C. P., 2005 and Fujarra, A. L. C., "The 'super-upper branch' VIV response of flexible cylinders", BBVIV4, June 2005, Santorini, Greece.
- [8] Pesce, C.P. and Fujarra, A.L.C., 2000, "Vortex-Induced Vibrations and Jump Phenomenon: experiments with a clamped flexible cylinder in water", *In. J of Offshore and Polar Engineering*, **10**, pp. 26-33.
- [9] Pesce, C.P., Martins, C.A. and Silveira, L.M.Y., 2006, "Riser-Soil Interaction: Local Dynamics at TDP and a Discussion on the Eigenvalue and the VIV Problems", *J Offshore Mechanics and Arctic Engineering*, **128**, pp.39-55.
- [10] Sarpkaya, T., 2003, "Critical Review of the Intrinsic Nature of Vortex Induced Vibrations". Naval Postgraduate School, Monterey, California, Report no. NPS-ME-03-002. 126 p.
- [11] Fujarra et al., 2001 "Vortex-Induced Vibrations of a Flexible Cantilever", *J Fluids and Structures*, **15** (3-4), pp. 651-658.
- [12] Herfjord K, Bryndum M, 2001, "Hydrodynamic interaction between two cylinders in steady flow", *11th International Offshore and Polar Engineering Conference*, **3**, pp. 237-243, Stavanger, Norway.
- [13] Sagatun SI, Herfjord K, Holmas T, 2002, "Dynamic simulation of marine risers moving relative to each other due to vortex and wake effects", *J Fluids and Structures*, **16** (3): 375-390.
- [14] Wu WS, Huang S, Barltrop, N, 2002, "Stationary and Hopf bifurcations of equilibrium positions of a cylinder situated in near and far wake fields of an upstream cylinder", *Int J Offshore and Polar Engineering* **12** (1): 31-33.
- [15] Huang, S. and Wu, W., 2003, "Nondimensional parameters governing the onset of wake-induced marine riser collision", *Proc. of the 22nd International Conference on Offshore Mechanics and Arctic Engineering*, Cancun, Mexico, June 2003.
- [16] Chaplin, J.R. et al, 2004, "Laboratory measurements of Vortex-Induced Vibrations of a vertical tension riser in a stepped current", *8th International Conference on Flow-Induced Vibration*, FIV2004, Paris, France, 6-9 July, 2004, **2**, pp. 279-284.
- [17] Alam, M.M., Moriya, M. and Sakamoto, H., 2003, "Aerodynamic characteristics of two side-by-side circular cylinders and application of wavelet analysis on the switching phenomenon", *J Fluids and Structures*, **18** (3-4), pp. 325-346.
- [18] Hamdan, B. A. et al., 1996, "Comparison of various basic wavelets for the analysis of flow-induced vibration of a cylinder in cross flow", *J Fluids and Structures*, **10** (6), pp. 633-651.
- [19] Lucor, D., Foo, J. and Karniadakis, G. E., 2005, "Vortex mode selection of a rigid cylinder subject to VIV at low mass-damping", *J Fluids and Structures*, **20** (4), pp. 483-503.
- [20] Bridge C., Howells H., Toy N., Parke G.A.R., Woods R., 2003, "Full-scale model tests of a steel catenary riser, *Fluid Structure Interaction II 03: Advances In Fluid Mechanics Series*, Eds. Chakrabarti S, Brebbia C, Almorza D, Gonzalezpalma R., **36**, 107-116.
- [21] Kaasen KE, 2002, "On identification of VIV modes from measurements", *12th International Offshore and Polar Engineering Conference*, **3**, pp. 827-833.